Chaos, noise, and tails on the I-V curve steps of rf-driven Josephson junctions

D. C. Cronemeyer, C. C. Chi, A. Davidson, and N. F. Pedersen*
IBM Thomas J. Watson Research Center, Yorktown Heights, New York 10598
(Received 14 August 1984)

We report the first experiments and digital and analog simulations which demonstrate the existence of chaotic regions in the I-V curves of dc- and rf-current-biased Josephson junctions. These junctions were formed of crossed Pb strips and were shunted with Au resistors. Chaos appears as negatively going tails on the trailing edges of the rf-induced steps; these tails, which may be as large as 50% of the voltage step width, have not previously been reported. The parameters for the occurrence of these tails center at $\beta_c=4$, $\Omega=\omega/\omega_p=0.15$, $i_{\rm rf}=I_{\rm rf}/I_c=1.04$, $I_c=3\times10^5$ A/m^2 at 4.2 K. The thermal noise of the shunting resistor was emulated by a Gaussian spectrum. The presence of such noise dramatically alters the substeps, spikes, and bifurcations predicted for zero temperature. With only small amounts of noise, such complexities disappear, and are replaced by a smooth tail on the step accompanied by broadband noise. There is good agreement between the experiments on a real junction, simulations with a phase-locked loop, and numerical calculations with a digital computer.

I. INTRODUCTION

Various wiggles and distortions of the I-V step structure induced by microwave irradiation incident upon Josephson junctions have been reported previously in the literature;[1-4] however, I-V curve distortions may occur even without microwave irradiation.[5] The "tails" on I-V steps which we discuss here have not been previously reported. For the most part, calculations[6-9] and experiments presented in the literature have been confined to rf bias alone as a function of various quantities such as the McCumber parameter[10] β_c, and the reduced frequency[10,4] Ω. It is worth noting in this connection that β_c may be nonzero for microbridges under certain circumstances.[11] Also, point contact Josephson junctions may have an appreciable point inductance which increases the complexity of their treatment.

Many studies on Josephson junctions have been related to the search for a dc-voltage standard composed of junctions whose specification would depend only upon fundamental atomic parameters such as the electron charge e and Planck's constant h, in addition to the driving frequency[12,13] ω. Few calculations have included the combined effects of dc and rf biases,[14-16] the situation most commonly encountered experimentally. Various "devils-staircase" structures,[17,18] substeps,[4,19,20] subharmonics,[21-23] and irregularities in the step structure of Josephson junctions have been predicted and some have been observed in experiments. The generation of subharmonics is of great conceptual interest since it indicates a more nonlinear or chaotic situation than for example in ordinary mixer devices where only standard harmonics and intermodulation frequencies are to be expected.

In this work, we have utilized both dc and rf current biases in conjunction with thermal (Gaussian) noise, since the actual Josephson junction is not operated at zero kelvin. The effects of noise are of great importance with regard to the actual phenomena to be observed, and cannot be ignored if realistic solutions are desired. Noise not only rounds the I-V curve features in general, but may completely remove spikes and substeps (and hence, subharmonics) from the picture.[18] By numerical simulation we can sort out the features which persist even with a noisy background from those which do not. In particular, we have observed tails on the rf-induced steps which have not been previously reported and which are not destroyed by an appropriate noise background according to our calculations. On the other hand, we find that only a few millikelvin equivalent of noise are required to completely destroy many spikes, substeps, and bifurcations to chaos, indicating why such sharp features have not been observed experimentally in the I-V curves of Josephson junctions.

II. METHODOLOGY AND EQUATIONS

The simple resistively shunted junction (RSJ) model[10,4,6] with current bias, rf drive, and Gaussian noise is depicted in Fig. 1(a). The equations relating these idealized parameters are written as

$$C\frac{dV}{dt}+R^{-1}V+I_c\sin\phi=I_{\rm dc}+I_{\rm rf}\sin(\omega t)+I_N\ , \quad \text{(1a)}$$

$$2eV=\hbar\frac{d\phi}{dt}\ , \quad \text{(1b)}$$

where C is the Josephson junction capacitance, V is the voltage across the junction, R is the shunting resistance, I_c is the critical current of the junction, ϕ is the phase difference across the junction, $I_{\rm dc}$ is the current drive, $I_{\rm rf}$ is the amplitude of the rf-current drive, and I_N is the Gaussian noise current equivalent to the thermal noise generated in the resistor R at a given temperature; in the Josephson relation (1b), e is the electron charge and $\hbar$ is Planck's constant divided by 2π. If we measure all currents in units of I_c and time in units of ω_p^{-1}, where $\omega_p=(2eI_c/\hbar C)^{1/2}=(L_JC)^{-1/2}$ is the plasma frequency,

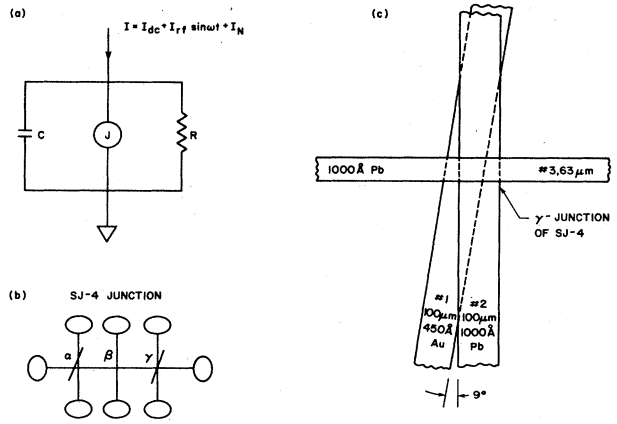

FIG. 1. (a) RSJ model. (b) A set of three junctions, two of which are shunted with Au resistors. (c) A blown-up picture of the γ-junction consisting of three layers: layer no. 1, 100 μm wide, 450 Å thick Au; layer no. 2, 100 μm wide, 1000 Å thick Pb; layer no. 3, 63 μm wide, 1000 Å thick Pb.

Eqs. (1a) and (1b) may be rewritten as

$$\frac{d^2\phi}{d\tau^2}+\beta_c^{-1/2}\frac{d\phi}{d\tau}+\sin\phi=i_{dc}+i_{rf}\sin(\Omega\tau)+i_N\ . \tag{2}$$

Here, $\beta_c=2eI_cR^2C/\hbar=R^2C/L_J$ is the McCumber parameter and L_J is the Josephson inductance ($\hbar/2eI_c$). It should be noted that some authors[10,12,13] use a normalization where time is measured in units of ω_c^{-1}, and $\omega_c=2eI_cR/\hbar=RL_J^{-1}$. It is useful to notice that $\omega_c/\omega_p=\beta_c^{1/2}$ in comparing literature citations. With this normalization to ω_c, Eqs. (1) have the form

$$\beta_c\frac{d^2\phi}{d\tau^2}+\frac{d\phi}{d\tau}+\sin\phi=i_{dc}+i_{rf}\sin(\Omega\tau)+i_N\ . \tag{3a}$$

Indeed, since there are three important frequencies in the case of the RSJ model, it is also possible to normalize the time unit as ω_a^{-1}, where $\omega_a=(RC)^{-1}$, in which case, Eqs. (1) become

$$\beta_c^{-1}\frac{d^2\phi}{d\tau^2}+\beta_c^{-1}\frac{d\phi}{d\tau}+\sin\phi=i_{dc}+i_{rf}\sin(\omega\tau)+i_N\ . \tag{3b}$$

These three frequencies arise naturally in connection with the $\omega-\beta_c$ diagram which will be discussed later, and it is to be noted that $\omega_a\omega_c=\omega_p^2$. It is also useful to note that $\beta_c=Q^2$, where Q is the quality factor for a Josephson junction (R/ω_pL_J in this case). We shall only make use of the plasma frequency normalization in this work.

It is worthwhile to note that the apparent second-order differential equation (2) can be written as two first-order equations (4):

$$\frac{dv}{d\tau}=\beta_c^{-1/2}[i_{dc}+i_{rf}\sin(\Omega\tau)-v-\sin\phi+i_N]\ , \tag{4a}$$

$$\frac{d\phi}{d\tau}=\beta_c^{1/2}v\ , \tag{4b}$$

and that these equations may be presented as an autonomous set (i.e., no explicit time dependence) by recognizing that $i=i_{dc}+i_{rf}\sin(\Omega\tau)+I_N$, and thus $di/d\tau=\Omega i_{rf}\cos(\Omega\tau)$. Hence, $\sin\Omega\tau=(i-i_{dc}-i_N)/i_{rf}$, and $di/d\tau=\Omega i_{rf}\ \{1-[(i-i_{dc}-i_N)/i_{rf}]^2\}^{1/2}$, and thus we have

$$\frac{dv}{d\tau}=\beta_c^{-1/2}(i-v-\sin\phi)\ , \tag{5a}$$

$$\frac{d\phi}{d\tau}=\beta_c^{1/2}v\ , \tag{5b}$$

$$\frac{di}{d\tau}=i_{rf}\Omega\{1-[(i-i_{dc}-i_N)/i_{rf}]^2\}^{1/2}\ . \tag{5c}$$

These three first-order equations could be represented as a single equation with derivatives no higher than third order in ϕ alone and with no explicit dependence upon the reduced time τ, but the resulting equation is of a complexity that makes it of little practical use:

$$\Omega^{-2}\left[\frac{d^3\phi}{d\tau^3}+\beta_c^{-1/2}\frac{d^2\phi}{d\tau^2}+\cos\phi\frac{d\phi}{d\tau}\right]^2+\left[\frac{d^2\phi}{d\tau^2}+\beta_c^{-1/2}\frac{d\phi}{d\tau}+\sin\phi-i_{dc}-i_N\right]^2=i_{rf}^2\ . \tag{6}$$

Since Eqs. (5) and (6) are in the autonomous form, however, the third-order differential equation character may be readily noted—an important theoretical feature for the development of "chaotic" solutions. Since for a second-order autonomous equation, trajectories in phase space do not cross, thus at least a third-order differential equation is required for chaos to occur.

III. EXPERIMENTAL CONDITIONS AND OBSERVATIONS OF TAILS ON THE MICROWAVE-INDUCED STEPS OF THE *I-V* CURVE

Evaporated crossed strips of Pb were utilized for the formation of the Josephson junctions studied in this work [Fig. 1(b)]. The actual junction size was $63\times100\ \mu m^2$; the barrier was provided by ambient oxidation of the Pb at approximately room temperature. The shunting resistor was provided by a Au stripe which was laid down first upon the c-axis polished quartz substrate by evaporation, and in the junction which we found to be of greatest interest, this Au stripe completely bridged the junction giving a very small inductance. The resistor value was thus determined by the two-dimensional spreading resistance of the two points at two of the four corners of the crossed Pb strips [Fig. 1(c)]. The samples were studied in the temperature range of 1.5 to 4.2 K. At 4.2 K, the critical current density was 2.7×10^5 A/m^2, and from this value we deduce[24] that the PbO_x barrier layer was 27 Å in thickness. If this oxide has a dielectric constant of 8.0, this corresponds with a capacitance of 170 pF. If we combine this value with that of I_c and $R=0.11\ \Omega$, for a microwave frequency of 3.86 GHz, we find $\beta_c=10$, $\omega_p=28$ GHz, and $\Omega=0.14$. On the other hand, the hysteresis[10] of the *I-V* curve ($\alpha_{cutoff}=0.5$) would lead one to expect $\beta_c=6$, for which (given the values above) we calculate a capacitance of 100 pF, $\omega_p=36$ GHz, and $\Omega=0.11$.

Therefore, we feel that these parameters should lie within the bounds $6<\beta_c<10$, $0.11<\Omega<0.14$.

If one utilizes a standard form of Ω-β_c diagram, then it may be noted that the sample is situated in the lower right-hand quadrant below the $\omega=(RC)^{-1}$ line in a region which has been designated as corresponding with "intermittent chaos"[12–16] (Fig. 2). The actual I-V curve data taken for such a junction is displayed at a normal scale in Fig. 3, and in a greatly expanded scale in Fig. 4. The voltage step spacing is about 8 μV; thus there is considerable experimental difficulty in avoiding drift and stray noise pickup in performing the experiment. EG&G 113 amplifiers were used as buffer amplifiers in making the measurements, and line voltage for the equipment was carefully regulated. The tails which appear prominently on certain of the I-V curve steps over some ranges of power input are clearly of unusual interest. The curves shown in Figs. 3 and 4 represent ascending traces only; both ascending and descending traces were recorded, however. The tails appear on both ascending and descending traces of the experimental curves, and are nearly reproducible from one run to the next. The appearance of the tails gives the impression that as the current is increased in order to pass from one step to the next, the voltage, instead of assuming an intermediate value between that of the one step and that of the next, instead tends to drop to zero. It is interesting to note that the tail amplitude usually follows a rule of "relaxation to the ohmic line." That is, when synchronization is lost in leaving the step, the tail usually extends toward the ohmic line—large amplitude tails occurring when the voltage difference of a step from the

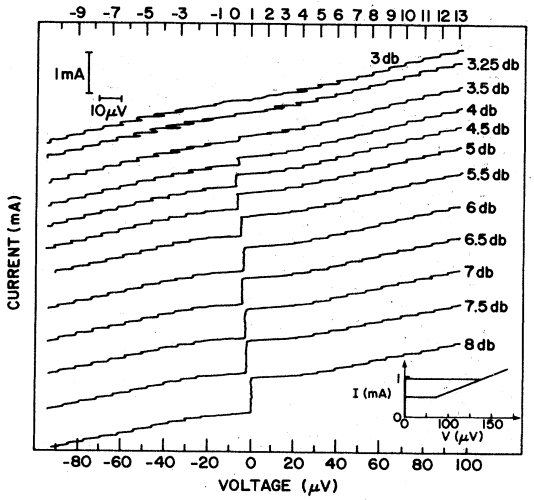

FIG. 3. Experimental I-V curves presented as a function of rf power for the SJ-4 at 4.2 K. The numbers at the top of the figure denote the order of each step. The inset shows the I-V curve for this junction with no rf power applied.

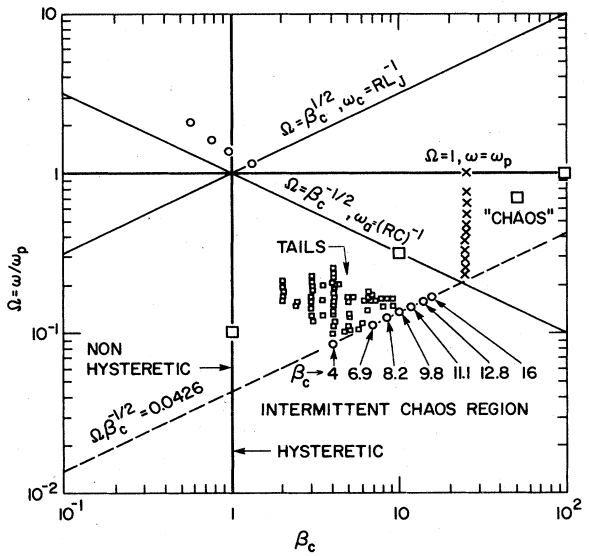

FIG. 2. Ω-β_c diagram with its major dividing lines arising from the three important frequencies under consideration; $\omega_1=RI_J^{-1}$, $\omega_2=\omega_p=(2eI_c/\hbar C)^{1/2}$, and $\omega_3=(RC)^{-1}$. The approximate boundary between hysteretic and nonhysteretic I-V curves is the line $\beta_c=1$. Chaos appears in the region bounded by $\Omega=1$ and $\Omega=\beta_c^{-1/2}$, intermittent chaos is found in the region bounded by $\Omega=\beta_c^{-1/2}$ and $\beta_c=1$. Tails are found in this region of intermittent chaos centering at $\Omega=0.15$, $\beta_c=4$ (small squares denote simulations). Detailed simulations are pursued in this paper for the line $\Omega\beta_c^{-1/2}=0.0426$ at the circled points on this line designated $\beta_c=4$, 6.9, 8.2, 9.8, 11.1, 12.8, and 16, with corresponding values of Ω. Results from other works of Huberman (Refs. 6 and 7) ($\beta_c=25$, various Ω), Kautz (Refs. 12 and 13) (large squares and the $\times$ at $\beta_c=25$, $\Omega=1$), Okuyama (Ref. 1) (small circles near $\beta_c=1, \Omega=1$), and Pedersen and Davidson (Ref. 8) (for $\beta_c=25$, $\Omega=0.3$ to 0.8 shown as $\times$'s) appear on the figure for reference.

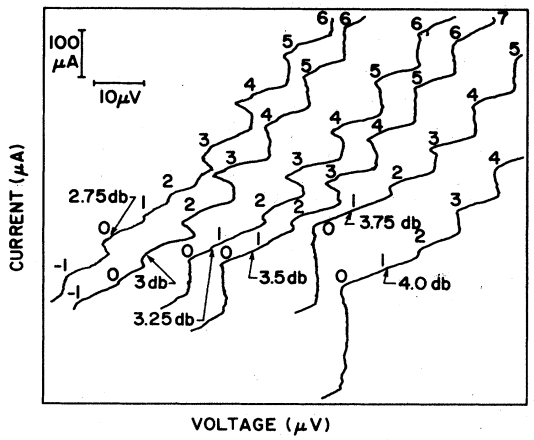

FIG. 4. A greatly magnified subset of the I-V curves for the same junction shown in Fig. 3.

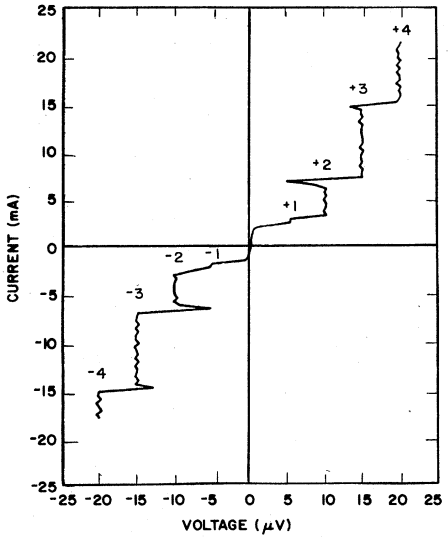

FIG. 5. A current-voltage curve set derived using the phase-locked-loop apparatus for $\beta_c=4$, $\Omega=0.16$, and $i_{\rm rf}=1.05$.

ohmic line is large. Sometimes the tail appears on the zero-order step, however, which would tend to make one doubt this explanation. Of course the matter is not really that simple, since noise rounding[18] also determines how closely the tail approaches this line. It is a subject of considerable interest[25–27] as to just how the transition is made from one ordered condition on step n to the ordered condition on step $n+1$—certainly, phase lock must be lost in the transition region, but without calculations it is not obvious how this takes place. Our simulations indicate that there are many ways for this transition to occur, but we shall concentrate here upon the one denoted as "negatively-going tails" for which we have experimental data in support of our calculations.

IV. ANALOG PHASE-LOCKED-LOOP SIMULATION OF THE RSJ MODEL

It has been realized for a long time that one may do an analog simulation of the Josephson junction by means of a phase-locked-loop subject to certain feed and scaling parameters.[28,29] Such an arrangement was set up for $\beta_c=4$, $\Omega=0.16$, $i_{\rm rf}=1.05$, and the I-V characteristic indicated in Fig. 5 was derived. The tails on the ends of the steps are clearly seen, and serve to confirm the reality of the experimental observations previously presented. An extensive analog study was not undertaken since it was felt that more detailed information would be available from the digital computer numerical simulations which will be discussed next.

V. DIGITAL COMPUTER SIMULATIONS OF THE RSJ MODEL WITH NOISE

Using Eq. (4) in its nonautonomous form, and expressing the differentials as finite differences for the numerical digital computer solution of the equation, we have

$$\Delta v=\beta_c^{-1/2}[i_{\rm dc}+i_{\rm rf}\sin(\Omega\tau)-v-\sin\phi+i_N]\Delta\tau\ , \tag{7a}$$

$$\Delta\phi=\beta_c^{1/2}v\,\Delta\tau\ . \tag{7b}$$

Various double-precision Fortran programs were written for use with a large digital computer; approximately 1000 time steps per rf cycle were used in these programs. The equations and analysis were so arranged that the Poincaré map could be obtained in addition to the usual phase maps, Fourier spectra of the power, and calculated I-V curves. Each point of the I-V curve was obtained after averaging over 1000 rf cycles. The Fourier spectra proved more useful than the Poincaré maps in clearly defining the periodicity at a given point of the I-V curve.

Now for Gaussian noise,[30–31] $\langle I_N\rangle_{\rm rms}=(4kT\,\Delta f/R)^{1/2}$. The bandwidth $\Delta f=(2eI_c/\hbar C)^{1/2}(2\Delta\tau)^{-1}$, where $\Delta\tau$ is the time-step employed in the numerical integration scheme. One can then write for this Gaussian noise distribution

$$\frac{\langle I_N\rangle_{\rm rms}}{I_c}=\langle i_N\rangle_{\rm rms}=(4ekT/\hbar I_c\Delta\tau)^{1/2}\beta_c^{-1/4}\ . \tag{8}$$

An extensive study was first made with the noise current set to zero (effectively $T_N=0$ K). It was ascertained that the negatively-going tails effect was noticeable in the region of $0.10\le\Omega\le0.22$, $2\le\beta_c\le10$, the tails seemed most pronounced for $\Omega=0.16$, $\beta_c=4$, $i_{\rm rf}=1.05$ (Fig. 2). Some of the steps calculated in this initial study had all kinds of complicated substructures, substeps, spikes, or critical points—sometimes of tremendous amplitude. An example is given in Fig. 6. The critical points frequently corresponded with periods of 3 or 5 times that of the rf drive period, and the substeps[17,19] were frequently of the form m/n if voltage is measured in terms of a normalized step width, and m and n are integers such as 2 and 3. Thus, one very elegant structure showed a transition from the $\frac{2}{3}$ to the $\frac{3}{2}$ step (Fig. 6). In addition, as one progressed toward the end of a voltage step, it was frequently observed that the oscillation traversed a sequence of period doublings so that periods of 2, 4, 8, 16, etc. were observed. This is indicated in Fig. 7, which shows phase maps and power spectra for such a sequence. Sometimes, unusual sequences such as 3, 6, 18, etc. were also observed.

Because of the extreme sharpness of these complicated spikes, substeps, and bifurcations, it is not unexpected[18] that they are affected by even a small amount of thermal noise introduced into the system ($T_N\neq0$). This is demonstrated in Fig. 8, which shows by numerical calculation how a complicated structure [e.g., Figs. 6(a) and 6(b)] with spikes, substeps, and bifurcation series develops into a smooth round tail as the amount of noise is increased. In fact, at temperatures as low as 50 mK, almost all of the fine structure is smoothed out, and between 1 and 9 K, the resulting I-V curve appears qualitatively just as was observed experimentally (Figs. 3 and 4), and by analog simulation (Fig. 5). To further investigate what may be expected in experiments at finite temperatures, we have calculated the noise spectrum corresponding to a thermally smoothed I-V curve for 4.2 K (Fig. 9). Notice that a large amount of noise is observed in the transition region

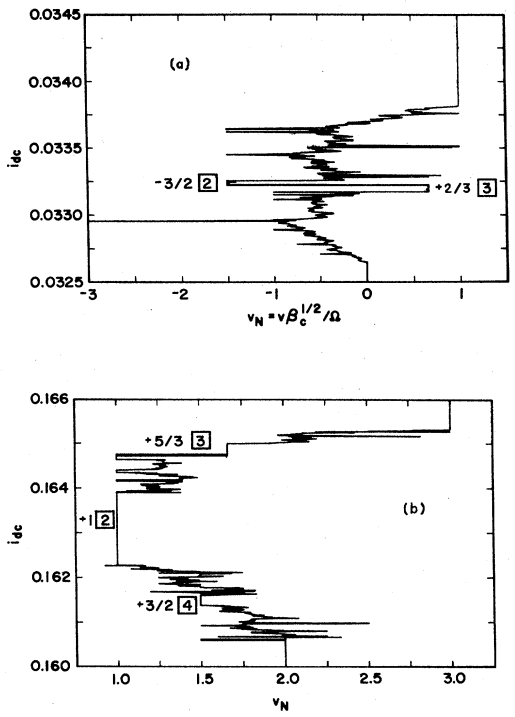

FIG. 6. Typical results of a numerical digital computer calculation for zero temperature, $\Omega=0.16$, $\beta_c=4$, $i_{rf}=1.05$ for (a) the zeroth step and (b) the second step. The numbers inside the squares denote the periodicity on the substep.

between the two rf-induced steps. Converted into an effective noise temperature, we find a maximum of approximately 10^4 K equivalent. We may note that in mixing experiments, unexplainably high noise temperatures are often found for bias points between two rf steps.[32] The calculations presented in Fig. 9 may point to the origin of that phenomenon.

VI. FITTING OF THE EXPERIMENTAL *I-V* CURVE DATA TO THE CALCULATED SHAPE USING DIGITAL COMPUTER SIMULATION

The experimental data for a Josephson junction at 4.2 K was introduced in Sec. III, and this data was digitized and the traces for ramping up and down were averaged in the process. A detailed average of step width was obtained from an analysis of all of the available step separations and this value was then used in conjunction with the microwave frequency as a check on the voltage calibration of the *X-Y* recorder; very good agreement was obtained. The problem with the matching of calculated and experimental curves is that the capacitance is not accurately known. However, knowing the area of the junction, and the properties of similar Pb-Pb junctions, it may be estimated that the capacitance is of the order of 170 pF, but this may be in error by as much as ±40%. However, if one specifies the critical current of the junction (which was accurately measured), the value of the shunting resistor (which could also be obtained accurately from the *I-V*

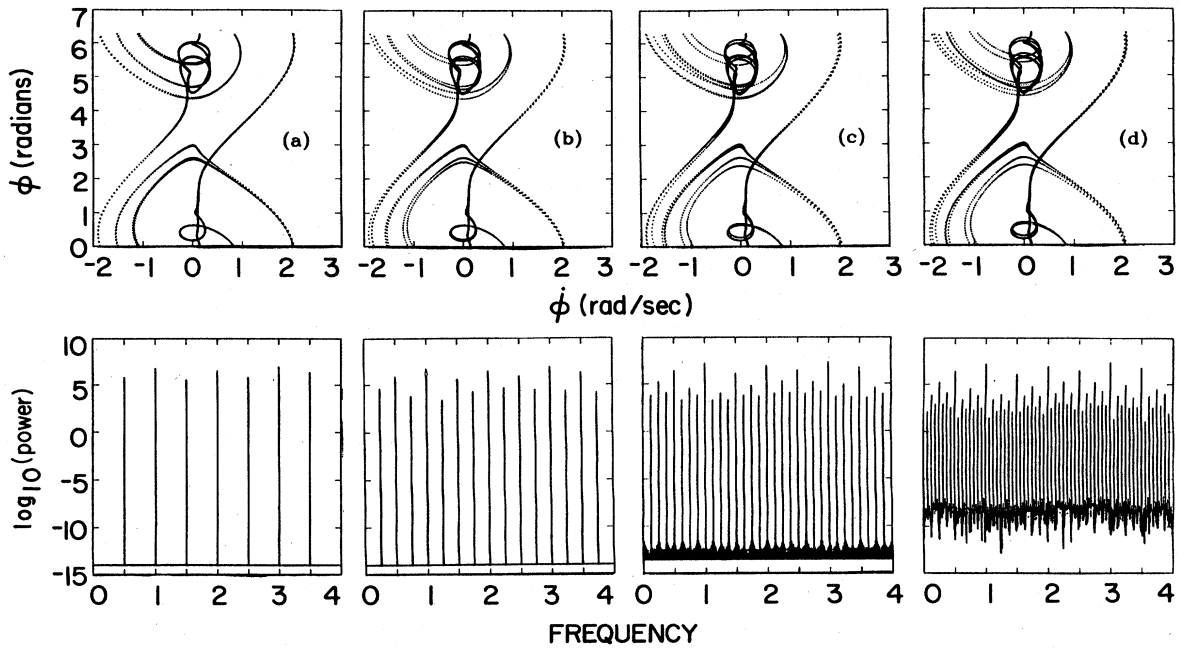

FIG. 7. A set of phase maps and Fourier spectra indicative of a bifurcation sequence as one approaches the trailing edge of a step showing periods of 2, 4, 8, and 16 times the drive period. The parameters are $\Omega=0.1$, $\beta_c=4$, $i_{rf}=1.05$, and $i_{dc}=$(a) 0.010 985 0, (b) 0.010 995 0, (c) 0.010 999 0, and (d) 0.011 000 0.

rigidly dictates the amount of the supercurrent so that there is little question that the attenuator setting derived spacings are inapplicable, so that the best fit to supercurrent values and tail magnitudes and shapes was found irrespective of the attenuator derived relative i_{rf} values. The correct order is preserved, of course, in this procedure, but the actual values of attenuation were ignored. Thus, a fairly good overall fit was obtained for the curves (c), (d), and (e) for i_{rf} values of 0.995, 1.010, 1.020, 1.030, 1.035, 1.060 (Fig. 11). Also, it may be noted that although the supercurrent variations and the tail amplitudes match reasonably well for this set of rf drive currents, the exact tail shape is not prefectly described. Experimentally, the tails are slightly "bulgy" ones, in that the voltage drops from the step value toward the axis, and then returns briefly to the step value before completing the transition to the next voltage step value—i.e., the tail is not quite at the very end of the step. This bulgy step behavior has been calculated to apply in the vicinity of $\beta_c \cong 11$, $\Omega \cong 0.14$ [curve (f) of Fig. 10], but a value of β_c this high seems unreasonable in deference to the observed hysteresis of the experimental I-V curves (inset to Fig. 3), although it agrees with our estimated capacitance in conjunction with the known R, I_c, and ω. Thus, one must conclude that for $\beta_c = 6.93$, $\Omega = 0.112$, a good semiquantitative fit is obtained to the experimental data using the simple RSJ model alone. Possible reasons for the RSJ model not yielding a totality of the experimental features observed are discussed later.

VII. DISCUSSION AND CONCLUSIONS

In this work, the experimental observation of tails on the I-V curve steps induced by microwave irradiation of a Josephson junction is confirmed by both analog and digital computer simulation. In the region of parameter space defined by reduced frequency $\Omega = 0.11$, $\beta_c = 6$, $i_{rf} = 1.05$, the I-V curve for a junction in passing from one step to another exhibits this unusual phenomenon which can be described as a negatively-going tail on the end of the voltage step. Perhaps the reason that this phenomenon has not been reported previously is simply that it occurs over a relatively narrow range of parameter space which has not been previously explored. Such tails are confined fairly closely to this vicinity in the Ω-β_c diagram, and outside this vicinity, different phenomena appear which are still under investigation. It was shown by digital computer simulation for zero noise temperature that in the approach to this tail region, bifurcation sequences obtain, and spikes (or critical bias points) and substep structures appear either before or mixed into the fully chaotic regions. Chaotic solutions are not unexpected for this third-order differential equation—see Eq. (6). However, with the addition of even a very small amount of thermal noise, most of the substructures are destroyed, all the spikes disappear, and the bifurcation sequences are unstable, thus the ordered system passes almost directly into a chaotic state characteristic of the tail region in general. Only the rounded-out tail shapes are predicted by the digital computer simulations with 4.2-K noise, in agreement with the experimental observations and the predictions from the analog phase-locked-loop experiment. With 4.2-K Gaussian noise, it is possible to obtain a reasonably good set of matches of the experimental I-V curves and their tails with that calculated by the digital computer simulation from the simple RSJ model alone. The marked difference in predicted behavior with and without thermal noise is one of the major achievements of this work. Certainly, many of the previous theoretical predictions which ignored the effects of noise can only be described as nonphysical.

The fact that the tail shape fitting is not perfect, however, can easily be noted since the tails on the steps as determined experimentally are not exactly at the ends of the steps—that is, as one nears the end of the step, the tail appears and then after rounding up from the tail, there is a slight tendency for the system to return to the step voltage before passing on to the next step voltage—a condition described as a bulgy step. This slight "bulginess" of the experimental tail data does not seem to be reproduced in the digital computer calculation of the straight RSJ model in reasonable parameter ranges of Ω and β_c. Bulges are noted, however, at high-order step numbers and for large drives for $10 \geq \beta_c \geq 15$, $0.14 \geq \Omega \geq 0.17$ in this work, and steps with bulges in the middle of the step has been found previously by simulation by Kautz[12,13] for $\beta_c = 25$, $\Omega = 1$. However, it is an important result of this study that the tails found experimentally are reproduced reasonably accurately from calculations based on the RSJ model alone.

It certainly may be conjectured that in the real physical situation, a very small inductance might be included in the shunt resistor for the Josephson junction. If the equations are written for this case, the fourth-order differential equation, equivalent to four first-order differential equations (autonomous form), would lead us to believe that, firstly, $\omega_p L/R$ is required to be exceedingly small, and hence L in the shunt resistor inductance must be extremely small in order to be negligible (~ 1 fH). Secondly, the effective R becomes larger, and hence the effective β_c becomes larger for a given set of R, C, ω, and thus the effective β_c might be higher than can be expected to agree with the measured dc parameters. This is readily seen if one thinks of the resistor arm as being composed of resistance plus inductive reactance as an indicator of the true behavior. This subject of an inductor in the resistive shunt arm across the junction is presently under investigation. With a geometry of the shunt other than that utilized in this work, the matter becomes of even more pressing importance. The presence of thermal noise has been shown to remove most of the sharp features of the I-V curves from Josephson junctions. However, it certainly would be fascinating to explore such junctions at temperatures below 1 mK, because there is theoretical prediction from the digital computer calculations that interesting substeps, subharmonics, critical bias points or spikes, and bifurcation sequences should become experimentally accessible.

ACKNOWLEDGMENTS

We wish to thank R. H. Koch for his advice concerning the noise treatment in this paper. R. B. Laibowitz and A. P. Malozemoff are also to be thanked for constructive criticism in assisting this project.

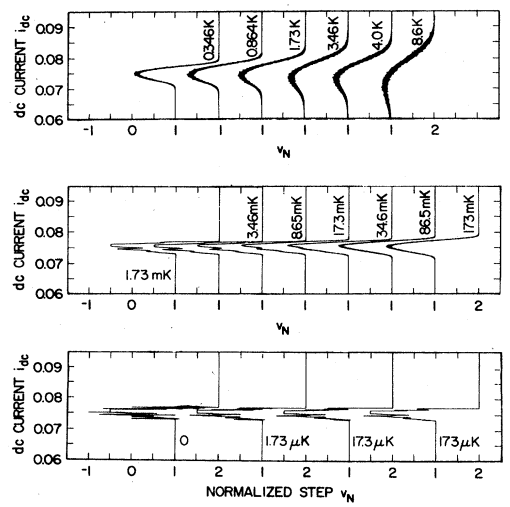

FIG. 8. Progress of a tail transition changing as a function of the noise temperature from $T=0$ to 8.6 K. The spikes disappear by 1 mK, and all substeps are gone by 35 mK, and from thence, the tail simply broadens and diminishes in amplitude with increasing temperature.

curve), and one knows the microwave frequency (3.86 GHz), then one readily finds that a line $\Omega\beta_c^{-1/2}=$const is defined, and for the parameters already specified, the constant is about 0.0426. Various combinations of Ω and β_c were then chosen along this line of the Ω-β_c diagram[12,13] (as plotted on logarithmic scales) which has a slope of $+\frac{1}{2}$ (Fig. 2). The choices of points are designated as circles along this line in the Ω-β_c diagram. Comparisons were then made between experimental and calculated *I-V* curves for various microwave power inputs (Fig. 10). An overall comparison of observed and calculated *I-V* curves is also shown (Fig. 11). The attenuator calibration of the microwave rf source (4.00, 3.75, 3.50, 3.25, 3.00, and 2.75 dB) would lead one to expect values of the i_{rf} equal to 0.927, 0.954, 0.982, 1.01, 1.04, and 1.07 (for curves A—F),

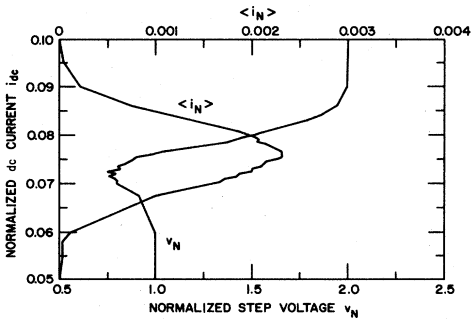

FIG. 9. Calculated appearance of noise as one passes through the tail region from step 1 to step 2 (parameters $\beta_c=4$, $\Omega=0.16$, $i_{rf}=1.05$). Note that the maximum noise appears to reflect the peak of dynamic resistance, but certainly is not the derivative of the tail curve.

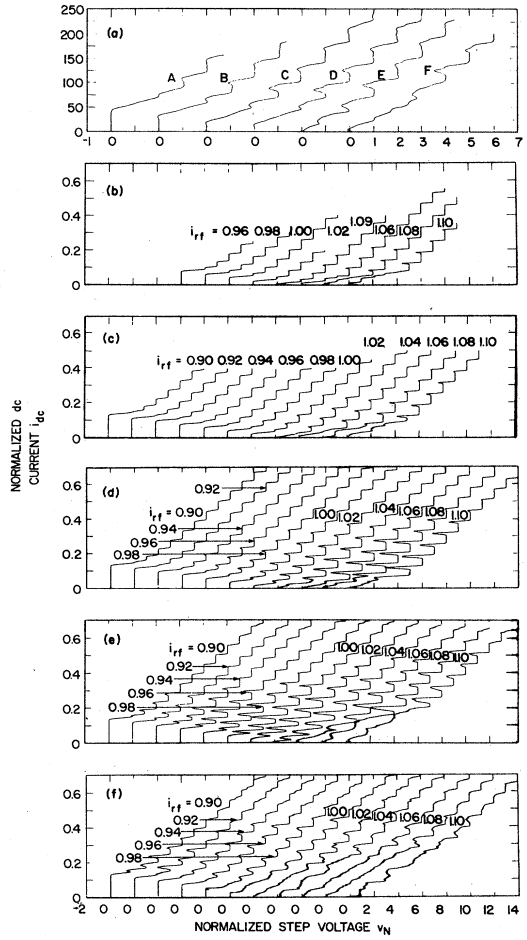

FIG. 10. A comparison of the experimental data for SJ-4 at 4.2 K (a) with calculated curves for $\beta_c=$(b) 6.25, (c) 6.9, (d) 8.2, (e) 9.8, and (f) 11.1, for corresponding values of Ω along the line $\Omega\beta_c^{-1/2}=0.0426$, and for various values of i_{rf} from 0.90 to 1.10.

in conjunction with the readily observable calibration point obtained for the supercurrent being driven to zero at $I_{rf}=1.04$ (curve E). It became obvious from a comparison of curves (b)—(f) of Fig. 10 that the match would be rather poor if this spread were correct. In fact, the rf drive

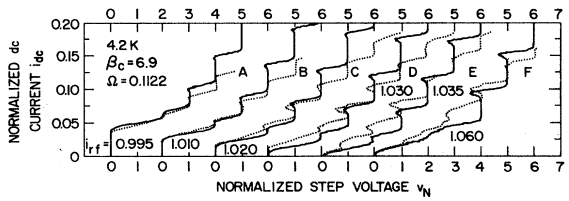

FIG. 11. A fit of the experimental data of SJ-4 (curves A—F) with $\beta_c=6.9$, $\Omega=0.1122$, and $i_{rf}=0.995$, 1.010, 1.020, 1.030, 1.035, and 1.060. Experimental curves are shown as the dotted lines, whereas the simulated curves are the solid lines.

*Permanent address: Physical Laboratory I, Technical University of Denmark, DK-2800 Lyngby, Denmark.
[1]K. Okuyama, H. J. Hartfuss, and K. H. Gundlach, J. Low Temp. Phys. **44**, 283 (1981).
[2]A. H. Dayem and J. J. Wiegand, Phys. Rev. **155**, 419 (1967).
[3]P. E. Gregers-Hansen, M. T. Levinson, and G. Fog Petersen, J. Low Temp. Phys. **7**, 199 (1972).
[4]N. F. Pedersen, O. H. Soerensen, B. Dueholm, and J. Mygind, J. Low Temp. Phys. **38**, 1 (1980).
[5]R. F. Miracky, J. Clarke, and R. H. Koch, Phys. Rev. Lett. **50**, 856 (1983).
[6]B. A. Huberman, J. P. Crutchfield, and N. H. Packard, Appl. Phys. Lett. **37**, 750 (1980).
[7]B. A. Huberman and J. P. Crutchfield, Phys. Rev. Lett. **43**, 1743 (1979).
[8]N. F. Pedersen and A. Davidson, Appl. Phys. Lett. **39**, 830 (1981).
[9]V. N. Gubankov, K. I. Konstantinyan, V. P. Koshelets, and G. A. Ovsyannikov, IEEE Trans. Magn. **MAG-19**, 637 (1983).
[10]D. E. McCumber, J. Appl. Phys. **39**, 3113 (1968).
[11]C. A. Hamilton and E. G. Johnson, Jr., Phys. Lett. **41A**, 393 (1972).
[12]R. L. Kautz, J. Appl. Phys. **52**, 3528 (1981); **52**, 6241 (1981).
[13]R. L. Kautz and G. Costabile, IEEE Trans. Magn. **MAG-17**, 780 (1981).
[14]E. Ben-Jacob, I. Goldhirsch, and Y. Imry, Phys. Rev. Lett. **49**, 1599 (1982).
[15]D. D'Humieres, M. R. Beasley, B. A. Huberman, and A. Libchaber, Phys. Rev. A**26**, 3483 (1982).
[16]W. J. Yeh and Y. H. Kao, Phys. Rev. Lett. **49**, 1888 (1982); Appl. Phys. Lett. **42**, 299 (1983).
[17]E. Ben-Jacob, Y. Braiman, and R. Shainsky, Appl. Phys. Lett. **38**, 822 (1981).
[18]Y. Braiman, E. Ben-Jacob, and Y. Imry, IEEE Trans. Magn. **MAG-17**, 784 (1981).
[19]O. H. Soerensen, N. F. Pedersen, J. Mygind, and B. Dueholm, J. Appl. Phys. **50**, 2988 (1979).
[20]J. Mygind, N. F. Pedersen, and O. H. Soerensen, Appl. Phys. Lett. **32**, 70 (1978).
[21]J. Mygind, N. F. Pedersen, O. H. Soerensen, B. Dueholm, and M. T. Levinson, Appl. Phys. Lett. **35**, 91 (1979).
[22]V. N. Belyk, N. F. Pedersen, and O. H. Soerensen, Phys. Rev. B **16**, 4853 (1977); **16**, 4860 (1977).
[23]N. F. Pedersen, M. R. Samuelson, and K. Saermark, J. Appl. Phys. **44**, 5120 (1973).
[24]S. Basavaiah, J. M. Eldridge, and J. Matisso, J. Appl. Phys. **45**, 457 (1974).
[25]M. J. Feigenbaum, J. Stat. Phys. **19**, 25 (1978); **21**, 669 (1979).
[26]H. J. Hartfuss and K. H. Gundlach, Phys. Didaktik **1**, 51 (1981).
[27]M. Cirillo and N. F. Pedersen, Phys. Lett. **90A**, 1509 (1982).
[28]C. K. Bak and N. F. Pedersen, Appl. Phys. Lett. **22**, 149 (1973).
[29]J. H. Magerlein, Rev. Sci. Instrum. **49**, 486 (1978).
[30]R. F. Voss, J. Low Temp. Phys. **42**, 151 (1981).
[31]Aldert van der Ziel, *Noise-Sources, Characterization, and Measurement* (Prentice-Hall, Englewood Cliffs, N.J., 1970), Chap. II, p. 10.
[32]J. H. Claassen and P. L. Richards, J. Appl. Phys. **49**, 4117 (1978).